10-1-2024

Transcription factor AP-2 gamma affects porcine early embryo development by regulating epigenetic modification.

Daoyu Zhang

Di Wu

Sheng Zhang

Meng Zhang

Yongfeng Zhou

See next page for additional authors

Authors

Daoyu Zhang, Di Wu, Sheng Zhang, Meng Zhang, Yongfeng Zhou, Xinglan An, Qi Li, and Ziyi Li

RBMO

ELSEVIER

ARTICLE

Transcription factor AP-2 gamma affects porcine early embryo development by regulating epigenetic modification

BIOGRAPHY

Li Ziyi is Professor at the First Hospital of Jilin University and Chief Scientist of the national key R&D project of China. His main research focus is reproductive development regulation and animal models of human diseases. He obtained the world's first somatic cell cloning ferrets.

Daoyu Zhang[a,1], Di Wu[b,1], Sheng Zhang[a], Meng Zhang[c], Yongfeng Zhou[a], Xinglan An[a], Qi Li[a], Ziyi Li[a,*]

KEY MESSAGE

The knockdown of TFAP2C inhibited porcine early embryonic development by regulating histone modification and DNA methylation. SETD2 and KDM5B were the main downstream genes influenced by TFAP2C. These results provided theoretical support for animal husbandry production.

ABSTRACT

Research question: What is the role and mechanism of action of transcription factor AP-2 gamma (TFAP2C) in porcine early embryo development?

Design: *TFAP2C* siRNA were injected into porcine oocytes, which subsequently underwent IVF. Different stages of embryos were collected for RNA sequencing, quantitative polymerase chain reaction, immunofluorescence staining to explore the affects in gene expression and epigenetic modification. Porcine fetal fibroblasts were transfected with siRNA, and cells were collected for chromatin immunoprecipitation and dual luciferase reporter assays.

Results: The deficiency of TFAP2C led to disorders in early embryonic development; 1208 genes were downregulated and 792 genes were upregulated in *TFAP2C* knockdown (*TFAP2C*-KD) embryos. The expression of epigenetic modification enzymes KDM5B, SETD2 were significantly elevated in the *TFAP2C*-KD group ($P < 0.001$). Meanwhile, the modification levels of H3K4me3 and H3K4me2 were significantly decreased ($P = 0.0021$, $P = 0.0029$), and H3K36me3 and DNA methylation were significantly increased in *TFAP2C*-KD group ($P = 0.0045$, $P = 0.0025$). DNMT1 was mainly expressed in nuclei in the *TFAP2C*-KD group ($P = 0.0103$). In addition, TFAP2C could bind to the promoter region of *SETD2*, and the mutation of the TFAP2C binding site resulted in increased activity of *SETD2* promoter ($P < 0.001$).

Conclusions: The knockdown of TFAP2C affects early embryonic development by regulating histone modification and DNA methylation.

[a] Key Laboratory of Organ Regeneration and Transplantation of Ministry of Education, First Hospital, Jilin University, Changchun 130021, China.
[b] First Hospital, Jilin University, Changchun 130021, China.
[c] The Jackson Laboratory for Genome Technology, 10 Discovery Drive Farmington, Connecticut, 06932, USA.
[1] Contributed equally.

*Corresponding author. E-mail address: ziyi@jlu.edu.cn (Z. Li). https://doi.org/10.1016/j.rbmo.2023.103772 1472-6483/
Declaration: The authors report no financial or commercial conflicts of interest.

KEYWORDS

TFAP2C
porcine embryo development
histone modification
DNA methylation
SETD2

INTRODUCTION

Embryonic development can be classified into several sequential stages that occur from the start of fertilization until the end of implantation: fertilization, morula and blastocyst formation. Understanding the stages of early embryo development and the underlying molecular mechanisms of regulation are essential for basic reproductive biology. Transcription factors control chromatin and transcription by recognizing specific DNA sequences. A previously published study has shown that transcription factors, such as OCT4, NANOG and SOX2, were expressed in the epiblast in pig (*Hall et al., 2009*). *Emura et al. (2019)* reported that *TEAD4* contributes to blastocyst formation in porcine embryos through the downregulation of *SOX2* expression. Research, however, is still required to fully understand the role f transcription factors in the early development of the pig embryo.

TFAP2C, a member of the AP-2 family, plays important roles in regulating cell development (*Pastor et al., 2018b*; *Wang et al., 2020a*). It has a canonical binding motif GCCNNNGGC. Previous studies have shown that *TFAP2C* is significantly induced during trophoblastic ectodermal differentiation in humans and murine. *Bai et al. (2012)* reported *TFAP2C* was one of the transcriptional regulatory circuitry transcription factors in humans, which is induced in trophectoderm and maintained in placenta. In mice embryos, however, Tfap2c is expressed in all cells of the morula, expression becomes restricted to the trophectoderm of late blastocysts and is co-expressed with *Cdx2* throughout extraembryonic ectoderm formation (*Kuckenberg et al., 2012*).*Winger et al. (2006)* reports that *TFAP2C* is expressed during mouse preimplantation embryonic development, is expressed in oocytes and declines sharply after fertilization, resumes expression at the four-cell stage and persists through the blastocyst stage. Moreover, *TFAP2C* is required for the survival of the mouse embryo. *TFAP2C* deficiency leads to mouse embryonic lethality at approximately embryonic day 7.5, which may be attributed to defective placental development (*Sharma et al., 2016*; *Wang et al., 2020a*). Studies of *TFAP2C* in porcine early embryo development, however, are limited.

Histone modifications are associated with the activation and repression of transcription. Earlier studies reported their functions in the regulation of transcription; for example, H3K4me1 (*Benevolenskaya, 2007*) and H3K4me3 (*Koch et al., 2007*) are associated with transcriptional activation, whereas H3K9me3 and H3K27me3 are associated with transcriptional repression (*Barski et al., 2007*). H3K4me3 is localized in the promoter region of the gene and is centred at the transcriptional start site (*Zardo, 2021*). In mouse embryonic stem cells, most transcription start sites are found to be tagged by H3K4me3 (*Bernstein et al., 2006*). In the same study, they found that H3K27me3 is more widely distributed, but that 75% of the H3K27me3 sites spanning the transcription start site are also labelled by H3K4me3 (*Bernstein et al., 2006*). In embryonic development, H3K4me3 leads to gene transcription from developing gametes to post-implantation embryos (*Zhang et al., 2016*). A previous study reports that the downregulation of H3K4me3 in full-grown oocytes by overexpression of the H3K4me3 demethylase KDM5B is associated with defects in genome silencing (*Zhang et al., 2016*).

Cytosine methylation in mammalian cells occurs mainly in CpG dinucleotides, and molecular and genetic studies have shown that DNA cytosine methylation (abbreviated as 5mC for 5-methylcytosine) is associated with gene silencing (*Moore et al., 2013*). DNA methylation is mainly established and maintained by DNA methyltransferases, which transfer a methyl group from S-adenyl methionine to the fifth carbon of a cytosine residue to form 5mC (*Chen and Zhang, 2020*; *Zhou et al., 2021*). DNMT1s are associated with metaphase II (MII) oocyte chromatin and are present in the nucleus throughout preimplantation development. Additionally, an interactive relationship exists between DNA methylation and histone modification (*Hashimoto et al., 2010*). Recent studies indicate that methylation of CpG islands relates to the methylation status of H3K4 (*Zardo, 2021*), and the levels of methylated H3K4 (H3K4me3) tend to be inversely correlated to DNA methylation (*Okitsu and Hsieh, 2007*).

Pigs are important agricultural livestock and a valuable animal model for xenotransplantation, disease models and basic biology research. Normal chromatin reprogramming is essential for embryonic development after fertilization, and it is believed that, in pig embryos, embryonic genome activation occurs at the four-cell stage (*Zhai et al., 2022*). In the present study, the key transcription factors that regulate embryo development were screened by analysing the expression pattern of transcription factors in porcine embryos. The function and mechanism of TFAP2C in regulating porcine embryonic development were investigated.

MATERIALS AND METHODS

Identification of and analysis of transcription factors

The RNAseq in vivo-fertilization (IVV) embryo data and MII oocyte data were previously uploaded to SRA NCBI database (https://www.ncbi.nlm.nih.gov/sra) with the accession number, PRJNA783716. Each of the three groups of IVV embryos at each of the four developmental stages (two cell, four cell, eight cell and blastocyst) was collected from a different sow by flushing out the embryos. Oocytes were collected from pig ovaries and matured *in vitro* to MII. All embryos and oocytes were washed by phosphate buffered saline (PBS) and then RNA was extracted by Trizol. The entire sequencing process of this experiment was commissioned to Beijing Novogene Biological Company (Beijing, China), including the extraction and quality control of RNA samples, cDNA amplification and library establishment, and computer sequencing. mRNA was purified from total RNA using poly-T oligo-attached magnetic beads. Fragmentation was carried out using divalent cations under elevated temperature in NEB Next First Strand Synthesis Reaction Buffer (5X). First strand cDNA was synthesized using random hexamer primers and M-MuLV Reverse Transcriptase. Second strand cDNA synthesis was subsequently carried out using DNA Polymerase I and RNase H. Remaining overhangs were converted into blunt ends via exonuclease and polymerase activities. After adenylation of the 3′ ends of DNA fragments, NEB Next Adaptors with hairpin loop structures were ligated to prepare for hybridization. To preferentially select cDNA fragments 150–200 bp in length, the library fragments were purified with an AMPure XP system (Beckman Coulter, Beverly, USA). Then, 3-μl USER Enzyme (NEB, USA) was used with size-selected, adaptor-ligated cDNA at 37°C for 15 min followed by 5 min at 95°C before

polymerase chain reaction (PCR). Then, PCR was carried out with Phusion High-Fidelity DNA polymerase, Universal PCR primers and Index (X) Primer. Finally, PCR products were purified (AMPure XP system) and library quality was assessed on the Agilent Bioanalyzer 2100 system. A cBot Cluster Generation System using TruSeq PE Cluster Kit v3-cBot-HS (Illumina, San Diego, CA, USA) was used to index-coded samples according to the manufacturer's instructions. After cluster generation, the library preparations were sequenced on an Illumina HiSeq platform and 125 bp/150 bp paired-end reads were generated. The accession IDs are as follows: MII_1 (SRR17041081), MII_2 (SRR17041080), MII_3 (SRR17041074), IVV_2C_1 (SRR17041073), IVV_2C_2 (SRR17041072), IVV_2C_3 (SRR17041071), IVV_4C_1 (SRR17041070), IVV_4C _2 (SRR17041069), IVV_4C_3 (SRR17041068), IVV_8C_1 (SRR17041067), IVV _8C_2 (SRR17041079), IVV_8C_3 (SRR17041078), IVV_Bla_1 (SRR17041077), IVV_Bla_2 (SRR17041076), IVV_Bla_3 (SRR17041075). Genes with false discovery rates (FDR) $\leq$0.01, |log2FC| $\geq$1.5 and $P \leq 0.01$ were selected as candidate genes. Transcription factor genes present in porcine oocytes and embryos were identified according to the list of transcription factor genes presented in **Supplementary Table 1**. The genes in the list were downloaded from TRRUST database (http;//www.grnpedia.org/trrust/). A heatmap of transcription factors identified in porcine MII oocytes and embryos was constructed by TBtools (https://bio.tools/tbtools).

Chemicals

All the chemicals used to culture were purchased from Sigma-Aldrich (St Louis, MO, USA) unless otherwise stated.

Collection and in-vitro maturation of porcine oocytes

The pig ovaries we used were all taken from the same local slaughterhouse (Changchun Huazheng, Jilin, China), and oocytes were transported to the laboratory within 2 h and were kept in 0.9% NaCl supplemented with 200 IU/m penicillin and streptomycin at 35–36.5°C.

The follicular fluid containing cumulus–oocyte complexes obtained from 3–6-mm ovarian follicles were aspirated using an 18-gauge needle. Cumulus–oocyte complexes with at least three layers of cumulus cells were selected, washed three times in manipulation fluid (TCM-199 supplemented with 0.1% polyvinyl alcohol) and then cultured in in-vitro maturation media. About 200 cumulus–oocyte complexes were each cultured in a 1-ml drop of maturation medium (TCM-199 supplemented with 10 μg/ml epidermal growth factor, 0.5 μg/ml porcine LH, 0.5 μg/ml porcine FSH, 26 mM sodium bicarbonate, 3.05 mM glucose, 0.91 mM sodium pyruvate, 0.57 mM cysteine, 0.1% PVA, 10% fetal calf serum, 75 mg/ml penicillin G and 50 mg/ml streptomycin) for 22–24 h and then cultured with hormone-free maturation medium (the formula is consistent with the previous maturation medium without 10 μg/ml epidermal growth factor, 0.5 μg/ml porcine LH and 0.5 μg/ml porcine FSH) for 20 h at 38.5°C and 5% CO_2. Then, cumulus cells were removed from oocytes with manipulation fluid supplemented with 0.2% hyaluronidase. The oocytes with polar body 1 (PB1) were considered matured and used for the following experiments.

TFAP2C siRNA screening

Porcine fetal fibroblasts cells were cultured in six-well plates with Dulbecco's Modified Eagle Medium (Gibco, MA, USA) supplemented with 10% fetal bovine serum (Gibco, Waltham, MA, USA) and 0.1% penicillin and streptomycin (volume per volume) at 37°C in 5% CO_2. The confluent degree reached 50–60% during transfection. Roche's siRNA transfection reagent was used: 2.5 μl transfection reagent was mixed with 47.5 μl opti-MEM mixture, and 1.89 μl siRNA was mixed with 48.1 μl opti-MEM mixture, and incubated at room temperature for 15 min, respectively. Then the two mixtures were combined and incubated at room temperature for 10 min. After completion, the mixture (total 100 μl) was added dropwise to the cells, and the samples were collected after 48 h of culture (37°C, 5% CO_2) for testing. The *TFAP2C* siRNA and negative control siRNA were designed and synthesized in Sangon biotech (Shanghai, China). The sequences were as followed:

TFAP2C siRNA1: sense: GCCCUGAUAG UCAUAGAUATT;
anti-sense: UAUCUAUGACUAUCAGGG CTT;
TFAP2C siRNA2: sense: CCGCACAGCA AGUGUGUAATT;
anti-sense:UUACACACUUGCUGUGCG GTT

NC: sense: UUCUCCGAACGUGUCA CGUTT;
anti-sense: ACGUGACACGUUCGGAG AATT.

Microinjection of oocytes

SiRNA was injected using a microinjecter (FemtoJet 4i (Eppendorf, Framingham, MA, USA). 5–10 pl of 25 nM *TFAP2C* siRNA (*TFAP2C* siRNA1) or negative control siRNA (a scrambled sequence of *TFAP2C*) were injected into MII oocytes, the oocytes of control group were not injected.

For rescue experiments, both *TFAP2C* siRNA and *KDM5B* siRNA or *SETD2* siRNA were injected into oocytes at the same time. The ratio of *TFAP2C* siRNA with *KDM5B* siRNA was 4:1, and the ratio of *TFAP2C* siRNA with *SETD2* siRNA was 2:1. The sequences were as followed: *KDM5B* siRNA2: sense: CCAACAGCAUAGCCAGAAATT; anti-sense: UUUCUGGCUAUGCUGUUGGTT; *SETD2* siRNA2: sense: GCACAUACUUCUGAUGAUUTT; anti-sense: AAUCAUCAGAAGUAUGUGCTT.

The *TFAP2C* mRNA was synthesized by MEGAscript^{TM}T7 kit (mMESSAGE mMACHINE^{TM}T7 ULTRA, AM1345), and 5–10 pl of mRNA was injected into oocytes using a microinjecter with a concentration of 910 ng/μl.

IVF of oocytes and embryo culture

Fresh semen was collected from the Jilin University pig farm. Semen samples were washed by density gradient centrifugation. In brief, 2-ml semen was added to percoll (Solarbio, Beijing, China) at concentrations of 90% and 45%, and centrifuged at 300 g for 20 min. After removal of the supernatant 4-ml Dulbecco's Phosphate-Buffered Saline (100 ml water with 800 mg NaCl, 20 mg KCl, 112 mg $Na_2HPO_4 \cdot 12H_2O$, 20 mg KH_2PO_4, 10 mg $CaCl_2$, 10 mg $MgCl_2 \cdot 6H_2O$, 100 mg bovine serum albumin [BSA]) was added and centrifuged at 300 g for 10 min. The spermatozoa were resuspended in porcine gamete medium (100 ml water with 0.6313 g NaCl, 0.07456 g KCl, 0.00477 g KH_2PO_4, 0.00987 g $MgSO_4 \cdot 7H_2O$, 0.2106 g $NaHCO_3$, 0.07707 g $CaC_6H_{10}O_6 \cdot 5H_2O$, 0.0187 g D-Glucose, 0.3 g PVA, 0.00242 g Cysteine, 0.04504 g $C_7H_8N_4O_2$, 0.0022 g $C_3H_3NaO_3$, and 100 μl/ml penicillin and streptomycin). A total of 60 MII oocytes (1 h after injecting siRNA) were incubated with spermatozoa in 400 μl porcine gamete medium, together with a final sperm concentration of 1.6×10^5 to 5.0×10^5 sperm/ml, at 38.5°C and 5%

CO_2 for 5–6 h. After washing off the adherent sperm, the fertilized oocytes were transferred to PZM-3 (50 ml water with 0.3156 g NaCl, 0.0373 g KCl, 0.0024 g KH_2PO_4, 0.0024 g $MgSO_4 \cdot 7H_2O$, 0.1055 g $NaHCO_3$, 0.0011 g Na-pyruvate, 0.0308 g Ca-[lactate]$_2 \cdot 5H_2O$, 0.0073 g L-glutamine, 0.0273 g hypotaurine, 0.15 g BSA, 1 mL BME amino acid, 0.5 Ml MEM non-essential amino acid). Embryos at the two-cell, four-cell and eight-cell stages were collected after culturing for 24 h, 48 h and 72 h in PZM3, respectively. The culture medium was changed to the PZM-3 with 10% fetal bovine serum after 5 days; the blastocysts were collected after 2 further days of culture.

RNA sequencing

Smart-Seq2 method was used to amplify each sample (six to eight IVF embryos at four-cell and eight-cell stages for each group) according to the manufacturer's instructions. RNA concentration of library was measured by Qubit 2.0 Fluorometer (Life Technologies, CA, USA). Agilent Bioanalyzer 2100 system was used to assess the insert size, and the quality of the amplified products was evaluated according to the detection results. Amplified product cDNA was used as input for the library construction of transcriptome. After the library construction, Agilent Bioanalyzer 2100 system was used to assess insertion size, and Taq-Man fluorescence probe of an AB Step One Plus Real-Time PCR system (Library valid concentration >10 nM) was used to quantify the accurate insertion size. A cBot cluster generation system and the HiSeq PE Cluster Kit v4-cBot-HS (Illumina, San Diego, CA, USA) were used to cluster the index-coded samples. Then, the libraries were sequenced by Zhejiang Annoroad Biotechnology (Beijing, China) on an Illumina platform, and 150 bp paired-end reads were generated. STAR (https://github.com/alexdobin/STAR/archive/2.7.3a.tar.gz) was used to compare transcriptome data and cuffLinks (http://cole-trapnell-lab.github.io/cufflinks/) for quantitative splicing. Differentially expressed mRNAs were identified by the IDEP website (http://bioinformatics.sdstate.edu/idep/). Genes with FDR ≤ 0.1, $|\log2FC| \geq 1.5$ and $P \leq 0.01$ were selected as candidate genes. The data are presented in **Supplementary Table 2**. Meanwhile, a heatmap of the DEG data was constructed according to the gene expression value by TBtools (Tbtools - CJchen's Blog (cj-chen.github.io)). The raw data are available in GEO database (GSE230288).

RNA isolation and quantitative polymerase chain reaction

Total RNA was extracted and complementary DNA (cDNA) was synthesized with SuperScriptTM IV CellsDirect^{TM} cDNA Synthesis kit (11750350) (Invitrogen, Carlsbad, CA, USA) following the manufacturer's instructions. Quantitative PCR was carried out with FastStart Essential DNA Green Master (06924204001) (Roche, Basel, Switzerland) via a StepOnePlus Real-Time PCR system. Primer sequences are presented in **Supplementary Table 3**.

The results were analysed using the $2^{-\Delta\Delta CT}$ method, and *GAPDH* is an internal reference gene. The quantitative PCR were all repeated three times.

Immunofluorescence staining

Embryos were washed with PBS containing 0.1% polyvinylpyrrolidone (PVP). The zona pellucida of embryos was dissolved in acidic Tyrode solution (pH 2.5). After washing in PBS–PVP, embryos were fixed with 4% paraformaldehyde for 30 min in the dark. After being washed in PBS-PVP, embryos were permeabilized with 0.2% Triton X-100/PBS (volume per volume) for 20 min and then blocked with 2% BSA and PBS for 1 h. For 5 mC/5 hmC staining, the embryos were treated with 4 M-HCl and Tris-HCl for 30 min each before BSA blocking. Embryos were incubated with primary antibodies overnight at 4°C. After being washed in PBS-PVP, embryos were stained with a second antibody at 37°C for 2 h in dark. Then DNA was stained with 10 μg/ml DAPI for 15 min.

For fetal fibroblasts, cells were washed three times with PBS and fixed with 4% paraformaldehyde at room temperature for 30 min. After washing three times with PBS, the cells were permeated with 0.2% Trition X-100 for 20 min and then closed in 1% BSA for 30 min. After washing with PBS for three times, the primary antibody was incubated at 4°C overnight, and the secondary antibody was incubated at room temperature for 2 h. Finally, DNA was stained with DAPI for 10 min.

The primary antibodies used in this study were as follofws: H3K4me2 (1:100, Abcam; ab7766; RRID:AB_2560996), H3K4me3 (1:100, Abcam; ab8580; RRID:AB_306649), and H3K9me3 (1:200, Abcam; ab8898; RRID:AB_306848), H3K36me3 (1:100, Bioss; bs-3768R; RRID:AB_10857890), SETD2 (1:100 Affinity, AF7552; RRID:AB_2843916), KDM5B (1:100, omnimabs; OM260516;), 5mC (1:100, Eurogentec; BI-MECY-0100; RRID:AB_2616058), 5hmC (1:100, Active motif; 39769; RRID:AB_10013602), DNMT1 (1:50, Thermo Fisher Scientific; MA5-16169; RRID:AB_2537688), FLAG (1:200,Thermo Fisher Scientific, MA5-15399, RRID:AB_10979908). The secondary antibodies were: Alexa Fluor 488 goat anti-rabbit (1:200, Invitrogen; A-11008;RRID:AB_143165), Alexa Fluor 488/594 goat anti-mouse (1:200, Invitrogen; A32723/A-11020; RRID:AB_2633275 / RRID:AB_2534087). The immunofluorescence staining was carried out with negative control (non-immune serum was used for the negative controls in place of the primary antibodies) when used for the first time; the negative control results are presented in **Supplementary Figure 4**.

All samples were observed under a Nikon Eclipse Ti-U microscope equipped with appropriate filters (Nikon, Tokyo, Japan) after mounting. Colour images were captured using a DS-Ri2 CCD camera (Nikon, Tokyo, Japan) and analysis software (NIS-Elements BR) (Nikon, Tokyo, Japan). The same exposure times and microscope settings were used for all captured images.

ImageJ software (National Institutes of Health, Bethesda, MD) was used to evaluate fluorescence intensity of individual images. A minimum of five embryos were analysed for stages in each group. The cytoplasmic background fluorescence intensity was measured as an average intensity level within the cytoplasmic area. Thereafter, the correction for the cytoplasmic background was carried out and the background-subtracted images were used for further analysis (*Zaitseva et al., 2007*). Simply, the first step is to split the fluorescence image into channels and retain the image that matches the fluorescence staining. Then, using the same threshold value, the fluorescence is localized to the cell nucleus, and the average fluorescence intensity is measured. All operations were carried out at room temperature unless otherwise specified.

Apoptosis assay on the blastocysts

At least five blastocysts were collected on the seventh day of incubation, the zona pellucida was removed by treatment with acidic Tyrode solution (pH 2.5) and embryos were fixed in 4% paraformaldehyde for 30 min. Fixed blastocysts were permeabilized for 30 min using 0.2% Triton X-100, washed three

times with PBS-PVP, and incubated at 37°C in the dark for 1 h with TdT (terminal deoxynucleotidyl transferase)-mediated dUDP nick-end labelling solution from the In Situ Cell Death Detection Kit (Roche, Basel, Switzerland). The embryos were washed three times with PBS-PVP and incubated for 10 min with DAPI to stain the nuclei. The stained embryos were mounted between a cover slip and a glass slide and examined under a fluorescence microscope.

Transfection of porcine fibroblasts

The day before transfection, 2×10^5 fetal fibroblasts were seeded into six-well plates to reach 30–40% confluence on the day of transfection. Cells were washed twice with pre-warmed PBS before transfection and 1 ml of medium without antibiotics was added according to the instructions and placed back in the incubator. Promage's plasmid transfection reagent was used in ratios of 4:1, 3:1 and 2:1, respectively, according to the instructions for pre-fixing; in the present transfection experiments, a ratio of 2:1 was used. The transfection reagent (0.4 μl), was mixed with plasmid (0.2 μg) in 8.64 μl opti-MEM mixture, then incubated for 15 min at room temperature. After completion, the mixture (total 10 μl) was added dropwise to the cells, and the samples were collected after 48 h culture (37°C, 5% CO_2) for testing.

Chromatin immunoprecipitation

Chromatin immunoprecipitation (ChIP) experiments were carried out according to the instructions (17-295) (Millipore, Boston, MA, USA) on porcine fetal fibroblast cells transfected with a high-expression plasmid containing a FLAG-tagged *TFAP2C* gene (pc-DNA3.1, RRID: Addgene_194725). Samples were collected after 48 h of transfection for ChIP assay. Four groups were set as input control, negative control, immunoglobulin control and Flag (fusion protein of TFAP2C and Flag). Finally, the DNA samples were amplified by PCR. JASPAR (https://jaspar.elixir.no/) was used for the prediction of the site of TFAP2C. The primers for PCR are presented in **Supplementary Table 4**.

Dual luciferase assay

The Promega kit was used for dual fluorescein assay by using porcine fetal fibroblast cells transfected with *SETD2* mut and *SETD* wild type plasmid (pGL4.1, RRID: Addgene_195037), following the manufacturer's instructions for the experiment, and the firefly and sea kidney fluorescence values were measured by enzyme marker; the firefly fluorescence value/sea kidney fluorescence value was the relative fluorescence intensity.

Statistical analysis

Data were presented as the means ± standard error of the means. The experiments were repeated at least three times in triplicate. GraphPad Prism 9.0.0 (GraphPad Software, Boston, MA, USA) was used for statistical analysis using t-test between the two sets of data, and one-way analysis of variance for more than two sets of data; pairwise comparisons were them conducted. $P < 0.05$ was considered statistically significant.

Ethical approval

The experimental protocol of this study was approved by the Animal Care and Use Committee of the First hospital of Jilin University on 25 February 2019 (reference number: 2019-099).

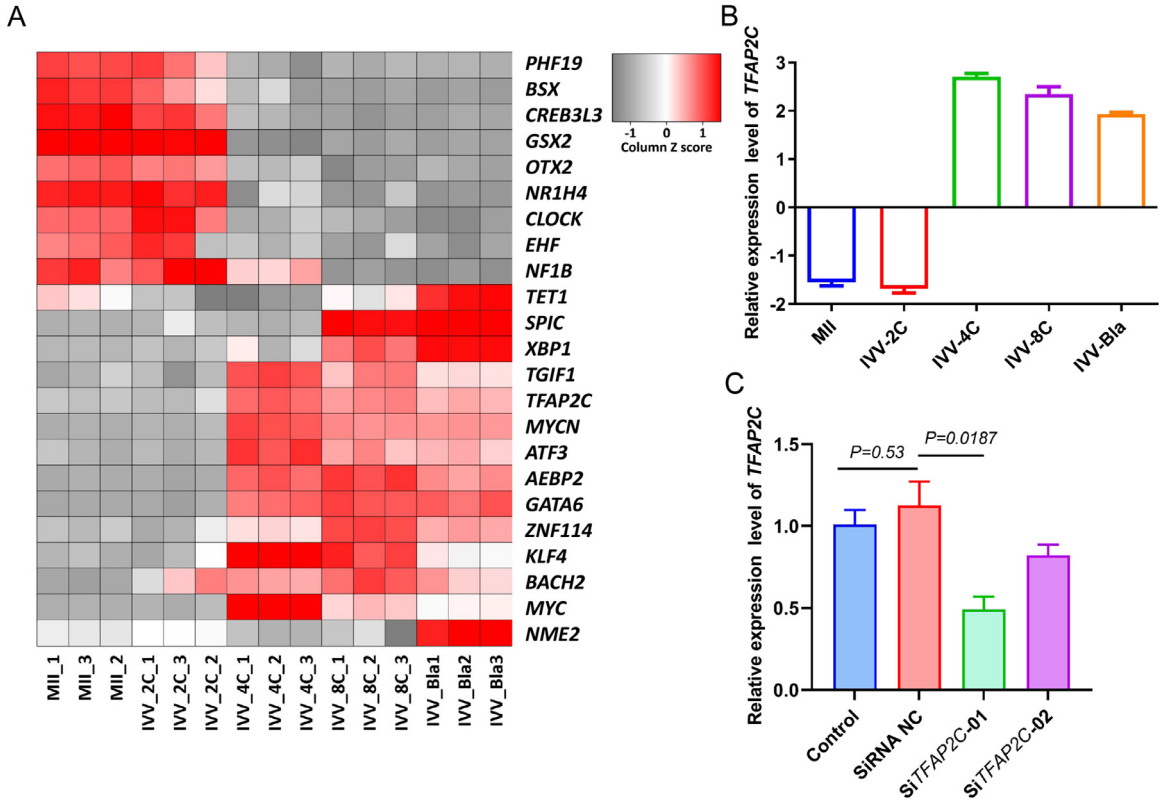

FIGURE 1 High expression level of TFAP2C in porcine embryos from four-cell to blastocyst. (A) The heatmap of transcription factors in pig metaphase II (MII) oocytes and in-vivo fertilization embryos; (B) the expression of *TFAP2C* in MII oocytes, and two-cell, four-cell, eight-cell and blastocyst stage in IVV embryos; (C) detection of interference effect of two *TFAP2C* siRNAs in transfected porcine fibroblasts. Data are presented as the mean ± standard error of the mean. T-tests were used to compare differences.

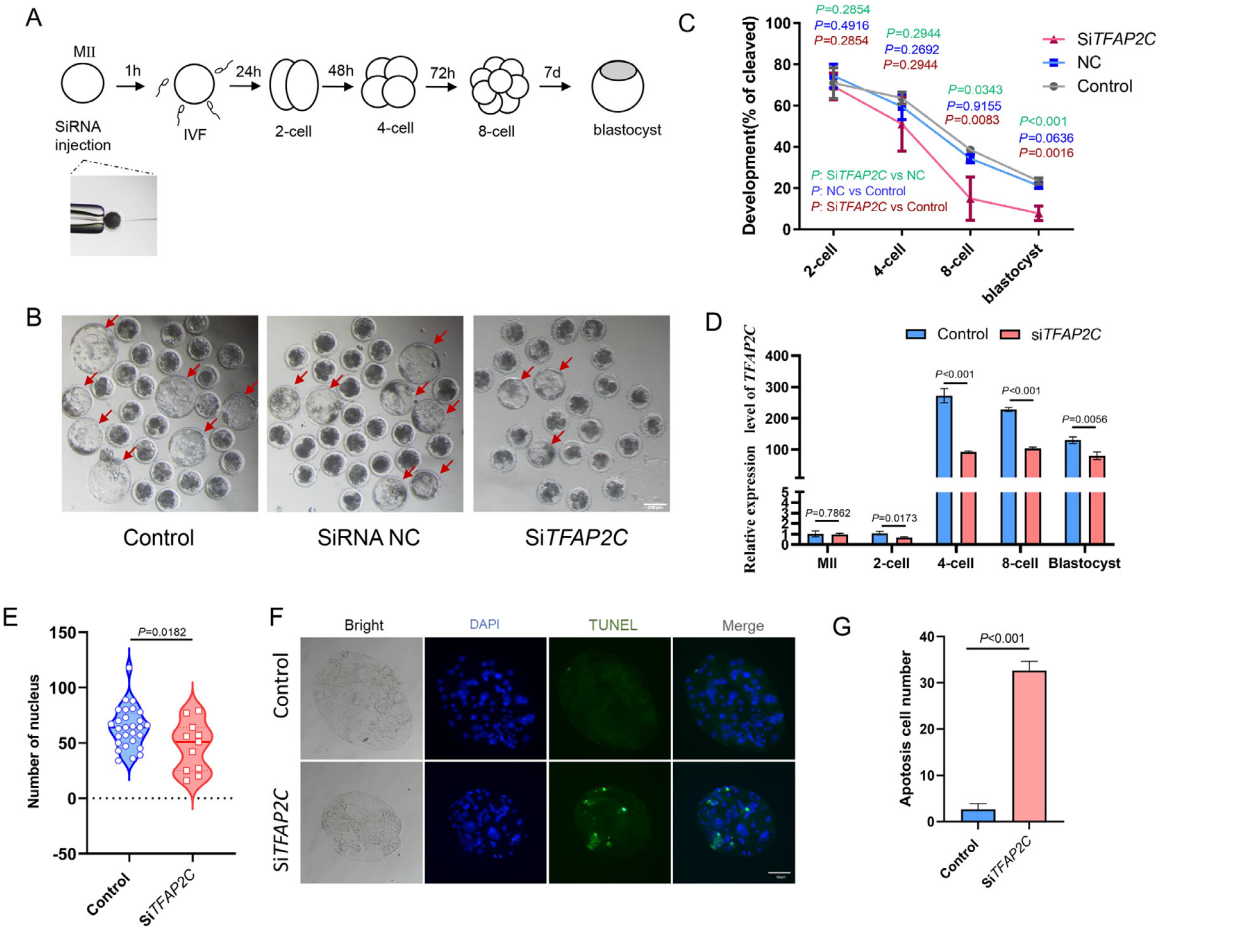

FIGURE 2 Interference with TFAP2C inhibited IVF embryo development. (A) Flow chart of interfering RNA injection and observation of early embryo development; (B) the three images were the blastocyst of control group, Si RNA negative control group and *TFAP2C*-KD group (Si*TFAP2C* group), respectively. The red arrow points to the blastocyst; (C) the embryonic development rate in two-cell, four-cell, eight-cell and blastocyst stage; *P*-value corresponds to control group versus Si*TFAP2C* group. The developmental rates of the control and negative control groups are also reported in *Zhang et al. (2022)*; (D) quantitative polymerase chain reaction analysis of *TFAP2C* relative expression of control and *TFAP2C*-KD groups at different development stages. Expression is relative to *GAPDH*. The experiment was independently repeated three times. Data are presented as the mean ± standard error of the mean in panels C and D; (E) the cell numbers of blastocysts in control group and *TFAP2C*-KD group; (F) The TdT (terminal deoxynucleotidyl transferase)-mediated dUDP nick-end labelling stain in blastocyst of control group and *TFAP2C*-KD group. The green indicates apoptotic cells. scale bar = 50 μm. The negative control is presented in **Supplementary Figure 4B**; (G) apoptosis cell number. The experiment was repeated three times independently with six to 10 embryos per stage per group per replicate. One-way analysis of variance were used to compare differences in panel C; the *P*-values in the figure show the *P*- values of Tukey's multiple comparisons test after one-way analysis of variance. T-tests were used to compare differences in panels D, E and G.

RESULTS

TFAP2C was upregulated from four-cell to blastocyst in porcine embryos

To search for key transcription factors during embryonic development, the RNAseq data of MII oocytes and IVV embryos, including two-cell, four-cell and eight-cell blastocysts, were analysed. The heatmap showed the expression pattern of transcription factors in IVV embryos (FIGURE 1A). Total number of genes was 23, among which nine genes (*PHF19*, *BSX*, *CREB3L3*, *GSX2*, *OTX2*, *NR1H4*, *CLOCK*, *EHF* and *NF1B*) were upregulated in oocytes and two-cell stage embryos, whereas they showed low expression in four-cell, eight-cell embryos and blastocysts. A total of 12 genes (*SPIC*, *XBP1*, *TGIF1*, *TFAP2C*, *MYCN*, *ATF3*, *AEBP2*, *GATA6*, *ZNF114*, *KLF4*, *BACH2* and *MYC*) showed low expression in oocytes and the two-cell stage, whereas they were unregulated in four-cell, eight-cell and blastocyst stages. From among these transcriptional factors, *TFAP2C* was the focus, because it was upregulated from the four-cell stage (FIGURE 1B) and because it has a classical DNA-binding motif. Next, two siRNA of *TFAP2C* were designed and transfected pig fetal fibroblasts with them and assayed their interference efficiency. As shown in FIGURE 1C, the *TFAP2C*-01 had a better interference effect ($P = 0.0187$); this siRNA was used in the following experiments.

The knockdown of *TFAP2C* inhibited porcine embryonic development

To investigate the function of *TFAP2C* in embryo development, *TFAP2C* siRNA was injected into the MII oocytes, which were subsequently fertilized *in vitro* (FIGURE 2A), and its effect on the embryonic development were investigated. Images of the resultant blastocysts are presented in FIGURE 2B. As shown in FIGURE 2C, no difference was observed in the percentage of the blastocysts between the siRNA negative control injected group (20.4 ± 0.95%) and the control group (22.92 ±

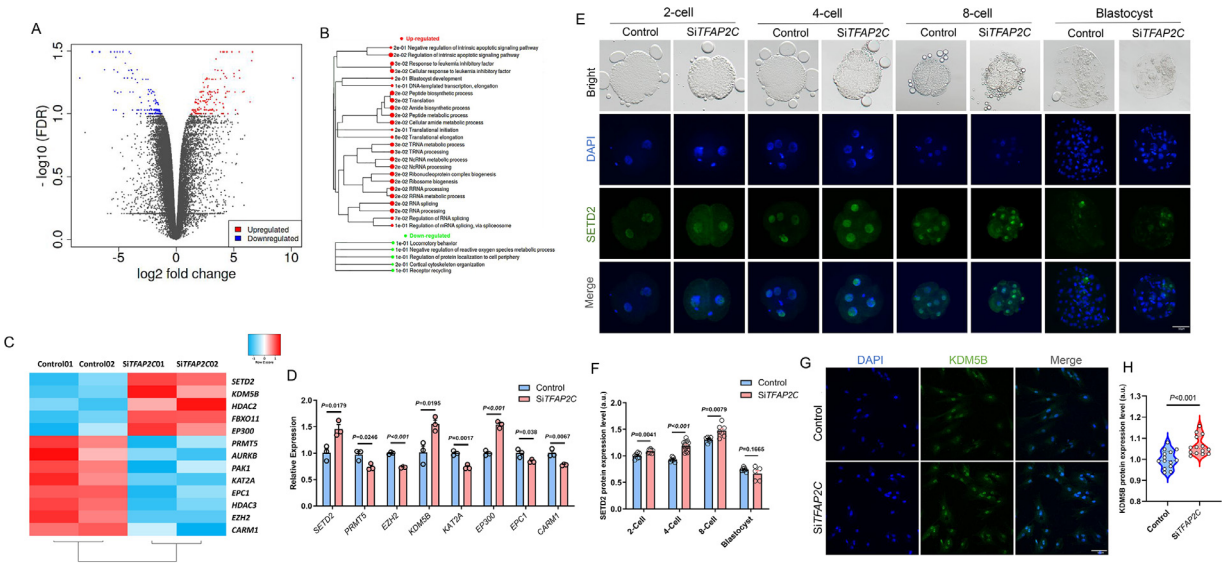

FIGURE 3 Interference with TFAP2C disrupted gene expression patterns. (A) The volcano shows differentially expressed genes between control group and *TFAP2C*-KD group (six to eight IVF embryos at four-cell and eight-cell stages in each group). Each dot represents a gene; the red dots indicate the upregulated gene and the blue dots indicate the downregulated genes; false discovery rate < 0.1, |log2FC| 1.5; (B) pathway enrichment of upregulated genes and downregulated genes; (C) heatmap of main epigenetic genes in control group and *TFAP2C*-KD group from RNA sequencing data (each sample includes six to eight IVF embryos at four-cell and eight-cell stages in each group). The colour scale bar was shown at the right of the heatmap. Blue indicated the lowest expression, and red indicated the highest expression; (D) the significantly changed epigenetic genes were detected by quantitative polymerase chain reaction in four-cell embryos. The experiment was independently repeated three times; (E) immunofluorescence of SETD2 in two-cell, four-cell, eight-cell and blastocyst. The nuclei (blue) were stained with DAPI. The experiment was repeated three times independently with five to 10 embryos per stage per group per replicate. scale bar = 50 μm. The negative control is presented in **Supplementary Figure 4A**; (F) fluorescence intensity analysis of SETD2; (G) immunofluorescence of KDM5B in fetal fibroblasts. The nuclei (blue) were stained with DAPI. The experiment was repeated three times independently. scale bar = 50 μm. The negative control is presented in **Supplementary Figure 4D**; (H) fluorescence intensity analysis of KDM5B. Data are presented as the mean ± standard error of the mean in panels D and F. The Solid line was the median and the dotted line was the interquartile range. T-tests were used to compare differences in panels D, H and F.

1.97%), suggesting no significant effect of negative control group. The percentage of the blastocyst in the *TFAP2C* knockdown (*TFAP2C*-KD) group (7.76 ± 1.86%) was significantly decreased compared with the control group ($P = 0.0016$). The developmental rates of the control and negative control groups are also reported in *Zhang et al. (2022)*. Meanwhile, the embryonic development difference was significantly changed from the eight-cell stage (FIGURE 2C) ($P = 0.0083$). As expected, *TFAP2C* levels were lower in *TFAP2C*-KD than in control group (FIGURE 2D) ($P < 0.001$ at four-cell stage). Fewer cell numbers ($P = 0.0182$) and more apoptotic cells in *TFAP2C*-KD blastocysts ($P < 0.001$) were observed (FIGURE 2E—2G). These data indicated that the knockdown of *TFAP2C* reduced the blastocyst formation and affected porcine early embryo development.

The knockdown of *TFAP2C* disturbed transcriptional reprogramming in embryos

To explore the regulatory mechanism of *TFAP2C* in porcine embryonic development, the four- to eight-cell stage of embryos were collected for RNAseq. As shown in FIGURE 3A, the volcano plot showed the differentially expressed genes between the control group and the *TFAP2C*-KD group: 1208 genes were downregulated and 792 genes were upregulated in *TFAP2C*-KD embryos. The function of these genes was analysed (FIGURE 3B); the upregulated genes were mainly enriched in the function of regulation of intrinsic apoptotic signalling pathway, peptide biosynthetic process, translation and amide biosynthetic process. The downregulated genes were enriched in negative regulation of reactive oxygen species metabolic process, regulation of protein localization to cell periphery, cortical cytoskeleton organization and receptor recycling. Epigenetic modification is crucial for the regulation of gene expression and the maintenance of cellular homeostasis, especially in embryo development. Therefore, genes related to the epigenetic modification (FIGURE 3C) were focused on, with the heatmap showing the expression pattern of primary epigenome genes. *SETD2* ($P = 0.0179$), *KDM5B* ($P = 0.0195$) and *EP300* ($P < 0.001$) were increased significantly, and *EZH2* ($P < 0.001$), *KAT2A* ($P = 0.0017$), *PRMT5* ($P = 0.0246$), *EPC1*($P = 0.038$) and *CARM1* ($P = 0.0067$) were significantly decreased (FIGURE 3D). These data revealed the knockdown of *TFAP2C* disturbed the transcription pattern during embryonic development and affected the expression of epigenetic modification genes.

SETD2 and KDM5B increased after *TFAP2C* knockdown

The expression of KDM5B, which is responsible for the demethylation of H3K4me3, and expression of the histone-lysine N-methyltransferase SETD2, were investigated by immunofluorescence. As shown in FIGURE 3E and FIGURE 3F, compared with the control group, SETD2 was significantly increased in two-cell ($P = 0.0041$), four-cell ($P < 0.001$) and eight-cell ($P = 0.0079$) stages after interfering with *TFAP2C*. The KDM5B expression in porcine fetal fibroblasts increased in the *TFAP2C*-KD group compared with the control group ($P < 0.001$) (FIGURE 3G and FIGURE 3H). These data indicated the knockdown of TFAP2C

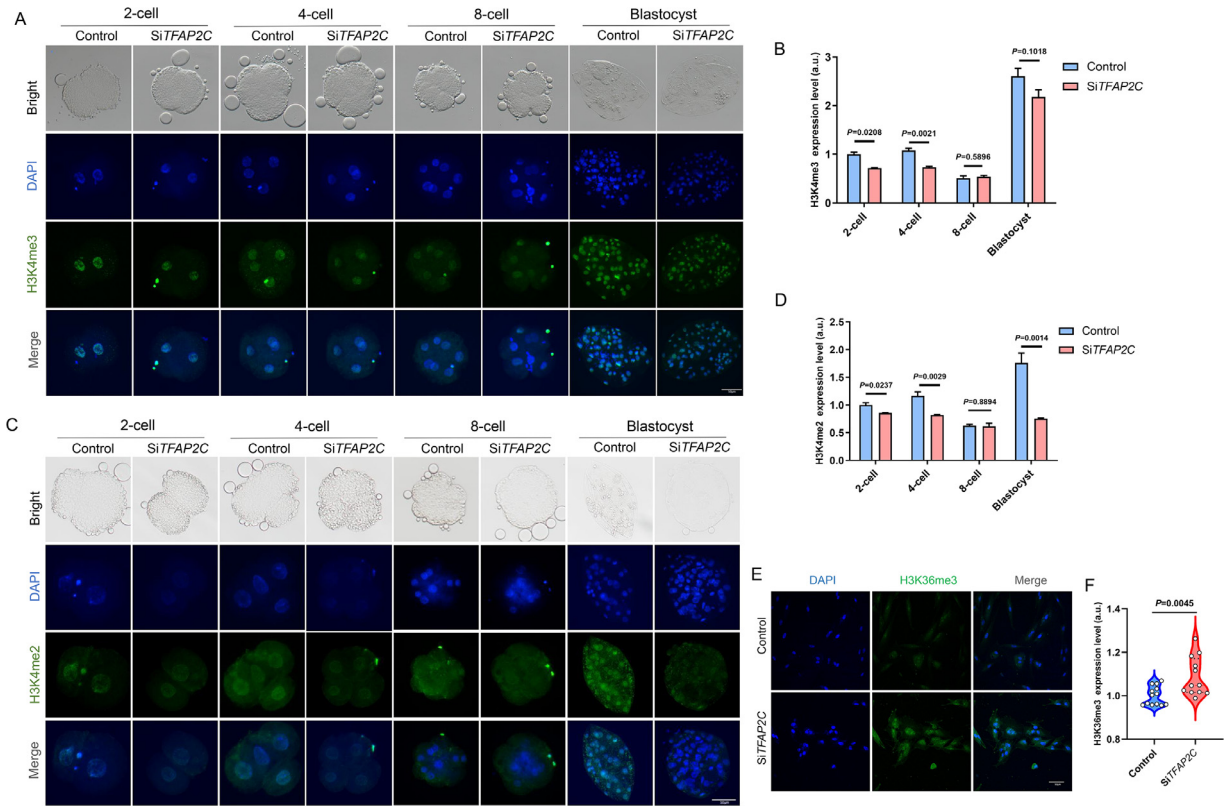

FIGURE 4 TFAP2C knockdown resulted in abnormal modifications of H3K4me3, H3K4me2 and H3K36me3. (A) Immunofluorescence of H3K4me3 in two-cell, four-cell, eight-cell and blastocyst. The nuclei (blue) were stained with DAPI. The experiment was repeated three times independently with six to 10 embryos per stage group per replicate. scale bar = 50 μm. The negative control is shown in **Supplementary Figure 4A**; (B) fluorescence intensity analysis of H3K4me3; (C) immunofluorescence of H3K4me2 in two-cell, four-cell, eight-cell and blastocyst. The nuclei (blue) were stained with DAPI. The experiment was repeated three times independently with six to 10 embryos per stage per group per replicate. scale bar = 50 μm. The negative control was shown in **Supplementary Figure 4A**; (D) fluorescence intensity analysis of H3K4me2; (E) immunofluorescence of H3K36me3 in fetal fibroblasts. The nuclei (blue) were stained with DAPI. The experiment was repeated three times independently. scale bar = 50 μm. The negative control was shown in **Supplementary Figure 4D**; (F) fluorescence intensity analysis of H3K36me3. Data are presented as the mean ± standard error of the mean in panels B and D. The solid line was the median and the dotted line was the interquartile range. T-tests were used to compare differences in panels B, D and F.

would induce the expression of SETD2 and KDM5B.

The knockdown of *TFAP2C* induced abnormal epigenetic reprogramming

Because of the abnormal expression of epigenetic genes in RNA sequencing, the primary histone modification level was investigated by immunofluorescence. The H3K4me3 modification level was investigated because KDM5B is a demethylase for H3K4me3. The immunofluorescence staining results showed that H3K4me3 was downregulated in the two-cell (P = 0.0208) stage and four-cell stage (P=0.0021) in the *TFAP2C*-KD group compared with the control group (FIGURE 4A and FIGURE 4B). H3K4me2 was downregulated in two-cell (P = 0.0237) stage, four-cell stage (P = 0.0029) and blastocyst (P = 0.0014) stage (FIGURE 4C and FIGURE 4D) in the *TFAP2C*-KD group. H3K4me3 is considered as an active transcriptional mark, whereas inhibitory histone modification H3K9me3 is typically associated with gene repression. The H3K9me3 immunofluorescence staining showed downregulated levels in the four-cell stage (P = 0.0019) and blastocyst in the *TFAP2C*-KD group (P < 0.001) (**Supplementary Figure 1**). Next, the modification level of H3K36me3 was detected in fetal fibroblasts. The results showed H3K36me3 was upregulated in the *TFAP2C*-KD group compared with the control group (P = 0.0045) (FIGURE 4E and FIGURE 4F).

To confirm the role of TFAP2C in epigenetic modification and embryonic development through SETD2 and KDM5B, rescue experiments were conducted. The results showed that the injection of interfering RNA effectively curtails the expression of *SETD2* (P = 0.0061) or *KDM5B* (P = 0.0014) in embryos (**Supplementary Figure 2A** and **Supplementary Figure 2C**). Notably, varied injection ratios demonstrated diverse effects on the expression of *SETD2* and *KDM5B* (**Supplementary Figure 2B** and **Supplementary Figure 2D**). The siRNA injection of *SETD2* with the ratio of 4:1 (P = 0.0240) or *KDM5B* with the ratio of 2:1 (P = 0.0362) can rescue the reduced blastocyst rate caused by *TFAP2C* deficiency compared with TFAP2C-KD group, respectively (FIGURE 5A and FIGURE 5C). This difference, however, still persists when compared with the control group (P = 0.0018 for *SETD2*, P = 0.0015 for *KDM5B*). In addition, the present results showed that elevated SEDT2 and abnormal H3K4me3 modification caused by *TFAP2C* deficiency can be rescued by injection of interfering RNA targeting SETD2 (P = 0.0450) (FIGURE 5D and FIGURE 5F) or interfering RNA targeting KDM5B (P = 0.0125) (FIGURE 5E and FIGURE 5G), respectively. Therefore, the knockdown of TFAP2C induced abnormal epigenetic modification.

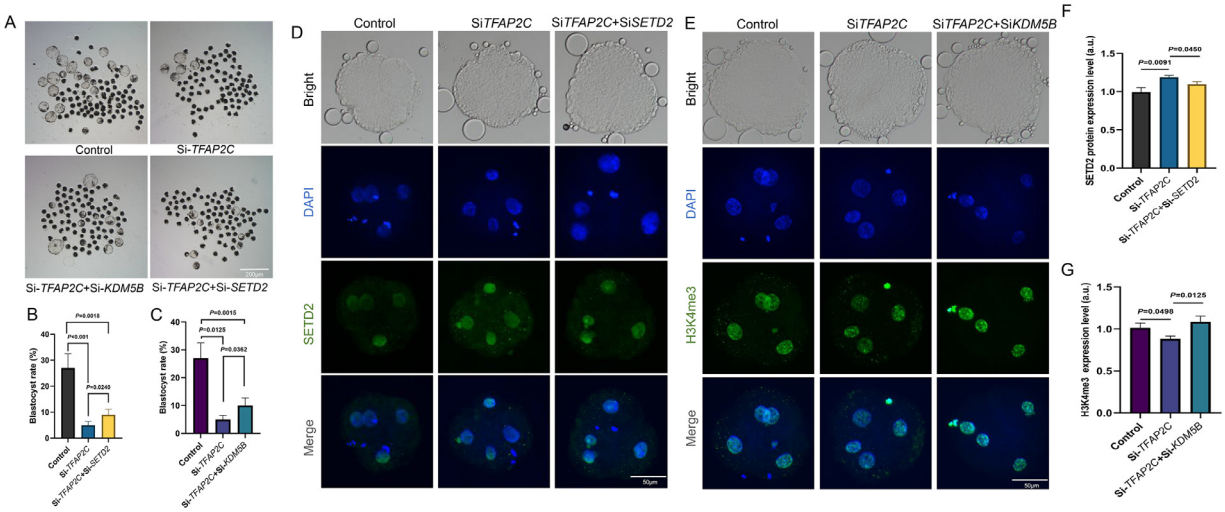

FIGURE 5 The interference of *SETD2* or *KDM5B* rescued the epigenetic modification caused by *TFAP2C*. (A) The developmental status of the blastocysts in each group. scale bar = 200 μm; (B) The blastocysts rate in control group, *TFAP2C*-KD group, both *TFAP2C* and *SETD2* interference group with a ratio of 4:1; (C) the blastocysts rate in control group, *TFAP2C*-KD group, both *TFAP2C* and *KDM5B* interference group with a ratio of 2:1; (D) immunofluorescence of SETD2 in four-cell embryos. The experiment was repeated three times independently with six to 10 embryos per group per replicate. scale bar = 50 μm; (E) immunofluorescence of H3K4me3 in four-cell embryos. The experiment was repeated three times independently with six to 10 embryos per group per replicate. Scale bar = 50 μm. The negative control is shown in **Supplementary Figure 4A**; (F) the normalized total fluorescence of SETD2; (G) the normalized total fluorescence of H3K4me3. Data are presented as the mean ± standard error of the mean in panels B, C, F and G. One-way analysis of variance was used to compare differences in panels B, C, F and G; the *P*-values in the figure show the *P*-values of Tukey's multiple comparisons test after one-way analysis of variance.

The knockdown of *TFAP2C* induced abnormal DNA methylation in porcine embryos

The methylation status of DNA is closely related to other epigenetic signals, including histone modifications, such as H3K4me3. Next, the 5 mC/5 hmC level was detected in embryos (FIGURE 6A), and immunofluorescence staining showed the 5 mC and 5 hmC levels in two-cell, four-cell, eight-cell and blastocyst stages. The 5 mC was upregulated in two-cell ($P = 0.0017$) and four-cell stages ($P = 0.0025$) (FIGURE 6B), suggesting abnormal DNA methylation modification occurred in *TFAP2C*-KD embryos. Meanwhile, the expression of DNMT1 was detected (FIGURE 6C and FIGURE 6D); the DNMT1 was mostly expressed in cytoplasm in the control group, whereas the DNMT1 was mostly expressed in nuclei in the *TFAP2C*-KD group ($P = 0.0103$). These data indicated the DNA methylation modification in *TFAP2C*-KD embryos was abnormal, in the absence of *TFAP2C*.

TFAP2C binds to the promoter of *SETD2*

To investigate how TFAP2C regulates the expression of epigenetic genes, the promoter region binding sites of epigenetic genes influenced by TFAP2C were predicted (FIGURE 3D) based on the canonical TFAP2C-binding motif GCCNNNGGC (FIGURE 7A). As shown in FIGURE 7B, the TFAP2C-binding motif GCCNNNGGC exists in the promoter regions of the epigenetic genes *SETD2*, *EP300*, *PRMT5*, *KAT2A*, *KDM5B*, *EZH2* and *CARM1*. Next, fetal fibroblasts were used to carry out chromatin immunoprecipitation (ChIP)-PCR to confirm which promoter was occupied by TFAP2C. As shown in FIGURE 7C, the promoter of *SETD2* was occupied with TFAP2C, indicating TFAP2C may regulate the expression of SETD2 by binding the promoter directly. Then, the classical pattern of TFAP2C in the *SETD2* promoter was mutated, and the results showed that the fluorescence activity of the wild-type group was significantly higher than that of the control group ($P < 0.001$), whereas the fluorescence activity of the mutant group was higher than that of the wild-type group (FIGURE 7D) ($P < 0.001$), suggesting that TFAP2C may function as a blocking protein. To further explore the regulatory effects of TFAP2C on *SETD2*, *TFAP2C* mRNA was synthesized and injected into oocytes that had been injected with siRNA. As shown in FIGURE 7E, the mRNA injection rescued the reduced expression of *TFAP2C* ($P < 0.001$). Next, the expression of *SETD2* was detected (FIGURE 7F [mRNA], FIGURE 7G [protein] and FIGURE 7H [protein]), and the SETD2 expression in the mRNA injection group was no different from the control group in mRNA level ($P = 0.1911$) and protein level ($P = 0.2151$). These data indicated TFAP2C could bind to the promotor of STED2 and restrict its expression.

High expression of TFAP2C had no significant effect on the expression of SETD2 and H3K36me3

To confirm the regulatory effect of *TFAP2C* on SETD2, TFAP2C was overexpressed, and its effect on SETD2 and H3K36me3 was observed. The expression of TFAP2C was detected after injecting the *TFAP2C* mRNA (**Supplementary Figure 3**), and the results showed TFAP2C was increased in the mTFAP2C group (mRNA injection group) compared with the control group ($P < 0.001$). The TFAP2C fusion protein expression was detected by immunofluorescence, which also increased in the mTFAP2C group in four-cell embryos (FIGURE 8A). No differences were found in SETD2 expression in embryos between the mTFAP2C group and the control group ($P = 0.4398$) (FIGURE 8B and FIGURE 8C). When H3K36me3 was detected in fetal fibroblasts, no significant differences were found between the control and *TFAP2C* mRNA injected group ($P = 0.0709$) (FIGURE 8D and FIGURE 8E). The overexpression of TFAP2C caused a decreased expression in *KDM5B* ($P = 0.0039$) and an increased modification level of H3K4me3 ($P < 0.001$) (FIGURE 8F–8H). These data indicated that

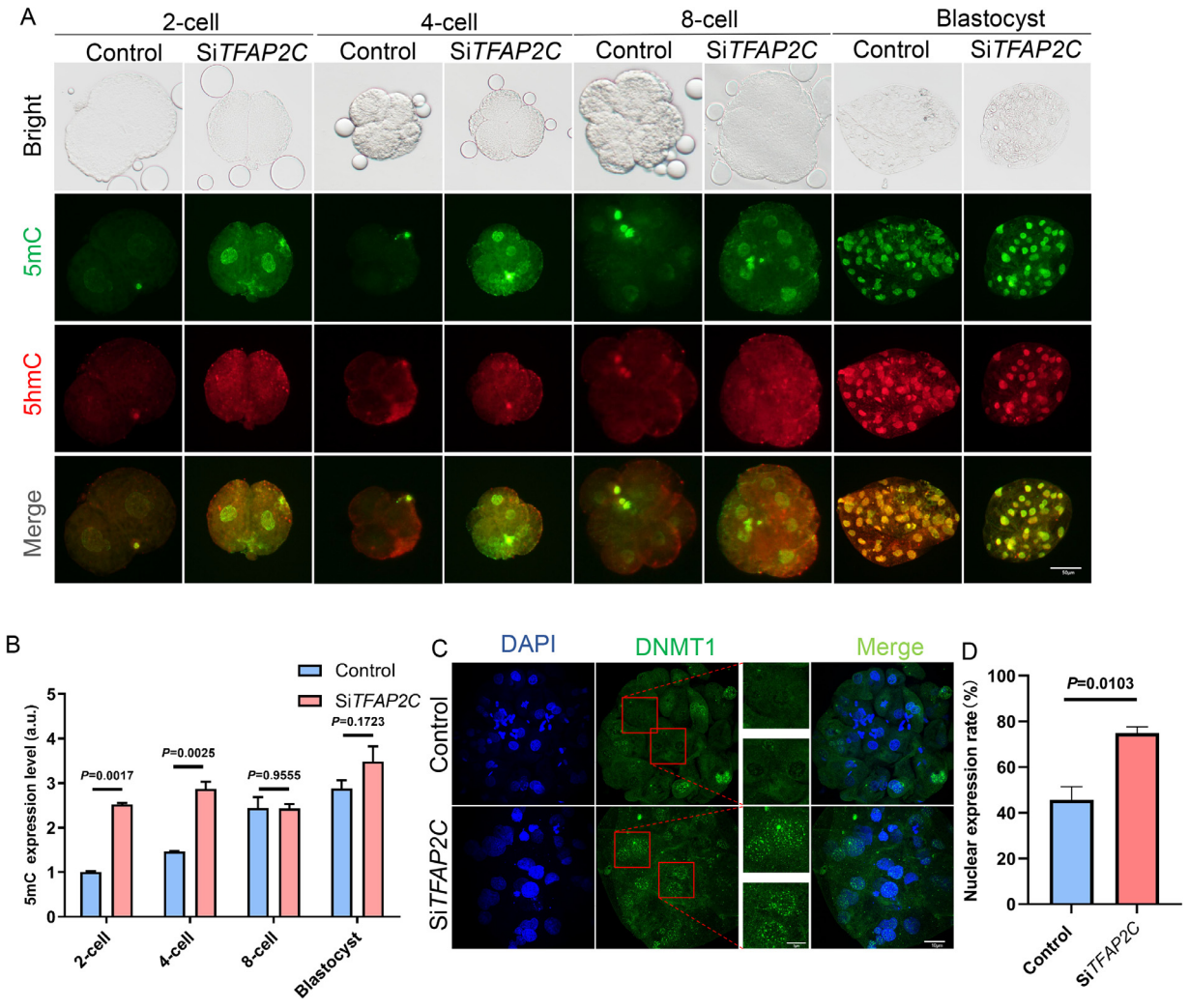

FIGURE 6 The knockdown of *TFAP2C* induced abnormal DNA methylation in embryos. (A) Immunofluorescence of 5 mC/5hmC in two-cell, four-cell, eight-cell and blastocyst. The green indicated 5 mC, and the red indicated 5 hmC. scale bar = 50 μm. The negative control is shown in **Supplementary Figure 4C**; (B) fluorescence intensity analysis of 5 mC; (C) immunofluorescence of DNMT1 in blastocyst. scale bar =10 μm, scale bar = 5 μm in the higher magnification. The negative control is presented in **Supplementary Figure 4A**; (D) fluorescence intensity analysis. The experiment was repeated three times independently with six to 10 embryos per stage per group per replicate. Data are presented as the mean ± standard error of the mean in panels B and D. T-tests were used to compare differences in panels B and D.

higher expression of TFAP2C could not affect SETD2.

DISCUSSION

Transcription factors are major developmental regulators that determine gene expression programmes, and understanding their role is one of the central goals of developmental biology (*Spitz and Furlong, 2012*). In the present study, an analysis of the expression patterns of significant transcription factors during embryonic development in pigs was conducted. The findings revealed a high degree of overlap between the activation time of most transcription factors and the time of zygotic genome activation. On the basis of this evidence, it has been speculated that these transcription factors may play a role in regulating gene expression and exert an effect on embryonic development.

TFAP2C promotes somatic cell reprogramming by inhibiting c-Myc-dependent apoptosis and promoting mesenchymal-to-epithelial transition (*Wang et al., 2020b*). In post-implantation embryonic development, it has been reported that *TFAP2C* knockout mice were developmentally delayed at 7.5 days and did not survive beyond 8.5 days compared with controls (*Auman et al., 2002*). *TFAP2C* in mouse pre-implantation embryonic development declines sharply after fertilization and begins to rebound at the four-cell stage (*Winger et al., 2006*). Whether *TFAP2C* deficiency affects preimplantation embryo development, however, was not investigated. *Aston et al. (2009)* found that *TFAP2C* was undetectable in oocytes and early embryos, whereas relatively high levels were detected in bovine IVF morula and blastocysts. Somatic cell nuclear transfer (SCNT) embryos expressed tfap2c at the eight-cell stage (*Aston et al., 2009*). In contrast, in pig parthenogenetic activation embryos, interfering with *TFAP2C* effectively inhibited the development of parthenogenetic activation embryos and blocked the embryos at the eight-cell stage

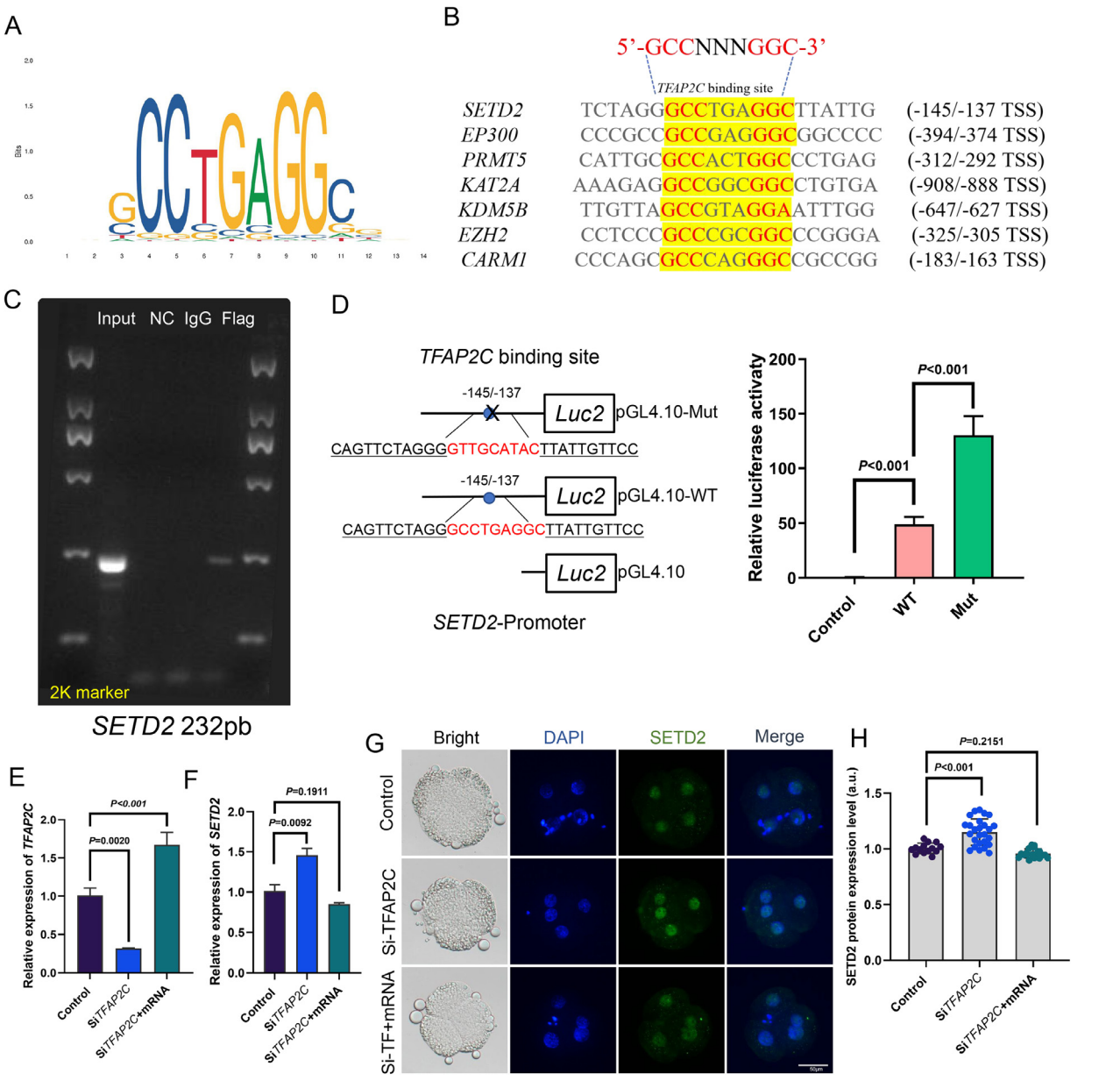

FIGURE 7 TFAP2C could bind to the promoter of *SETD2*. (A) The classical binding motifs of TFAP2C; (B) prediction of promoter binding sites in epigenetic genes those influenced by TFAP2C in FIGURE 3D. Porcine fetal fibroblast cells transfected with a high-expression plasmid containing a FLAG-tagged *TFAP2C* gene were investigated; (C) the result of chromatin immunoprecipitation assay; the lanes from left to right were input, negative control (NC), immunoglobulin (IgG) and Flag; (D) dual luciferase reporter experiment showing pGL4.10 vectors with wild type (WT), mutant (mut) *TFAP2C* in *SETD2* promotor or no promotor (control); (E) quantitative polymerase chain reaction analysis of *TFAP2C* expression in control group, *TFAP2C*-KD group (SiTFAP2C) and the *TFAP2C* siRNA plus *TFAP2C* mRNA injection group (four-cell stage, $n = 30$ per group). The experiment was independently repeated three times; (F) quantitative polymerase chain reaction analysis of *SETD2* expression (four-cell stage, $n = 30$ per group). The experiment was independently repeated three times; (G) immunofluorescence of SETD2 at four-cell stage. The nuclei (blue) were stained with DAPI. scale bar = 50 μm; (H) fluorescence intensity analysis. The experiment was repeated three times independently with six to 10 embryos per stage per group per replicate, $P < 0.001$. Data are presented as the mean ± standard error of the mean in panels F and H. One-way analysis of variance was used to compare differences in panels D, E, F and H; the *P*-values in the figure show the *P*-values of Dunnett's multiple comparisons after one-way analysis of variance. TSS, transcription start site.

(*Lee et al., 2016*). These results indicate that the expression pattern of *TFAP2C* varies at different developmental stages. In the present study, *TFAP2C* expression was elevated starting at the four-cell stage of porcine embryos and persisted until the blastocyst stage. Interfering with *TFAP2C* effectively inhibited the developmental efficiency of porcine embryos, and with significant differences at the eight-cell stage and induced apoptosis, indicating the normal expression of *TFAP2C* in porcine embryos in necessary. Further research into mechanisms is needed.

Histone modifications play a key role in the spatial and temporal regulation of mammalian gene expression (*Bannister*

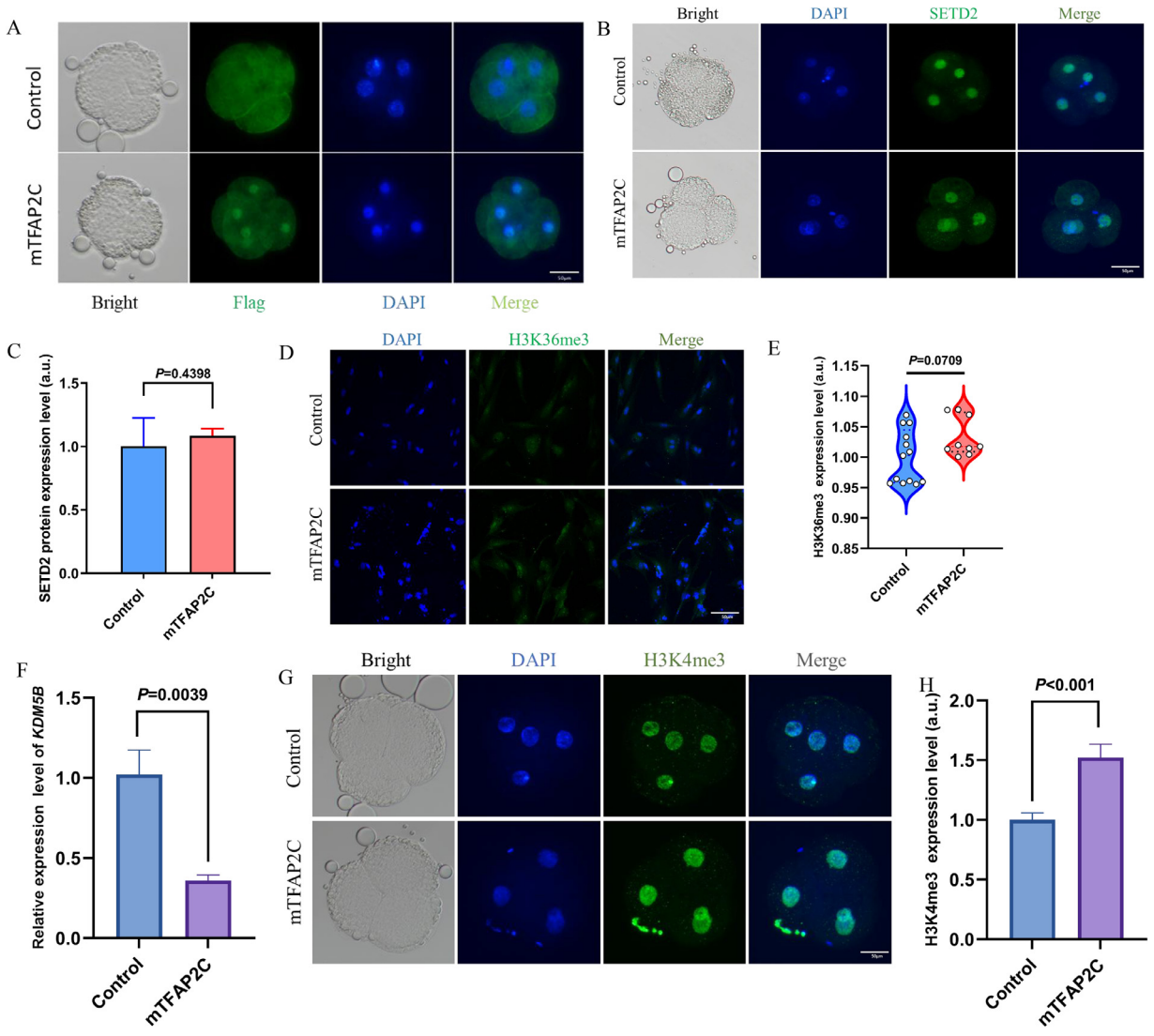

FIGURE 8 High expression of TFAP2C had no significant effect on the expression of SETD2 and H3K36me3. (A) Immunofluorescence of fusion protein of TFAP2C (Flag) in four-cell stage embryos. The experiment was repeated three times independently with six to 10 embryos per group per replicate. scale bar = 50 μm; (B) immunofluorescence of SETD2 in four-cell stage. The experiment was repeated three times independently with six to 10 embryos per group per replicate. scale bar = 50 μm; (C) fluorescence intensity analysis of SETD2; (D) immunofluorescence of H3K36me3 in fetal fibroblasts. The nuclei (blue) were stained with DAPI. The experiment was repeated three times independently. scale bar = 50 μm; (E) fluorescence intensity analysis of H3K36me3. The solid line was the median and the dotted line was the interquartile range; (F) quantitative polymerase chain reaction analysis of *KDM5B* in the control group and TFAP2C over-expression group in embryos (four-cell embryos); (G) immunofluorescence of H3K4me3 in four-cell embryos. The experiment was repeated three times independently with six to 10 embryos per group per replicate. Scale bar = 50 μm; (H) fluorescence intensity analysis of H3K4me3, $P < 0.001$. Data are presented as the mean ± standard error of the mean in panels C, F and H. T-tests were used to compare differences in panels C, E, F and H.

and Kouzarides, 2011). *Shao et al. (2008)* reported that the increased expression of H3K4me2 at two-cell stage caused abnormal activation of embryonic gene expression and further reduction of developmental efficiency in mice. The abnormal modification of H3K4me3 was correlated with abnormal gene expression in extraembryonic tissues (*Bai et al., 2022*). SETD2 is an H3K36me3 methyltransferase (*Xu et al., 2019*), previous studies have demonstrated that SETD2 is expressed in pig embryos, and its expression patterns differ among parthenogenetic activation, IVF, and SCNT embryos (*Diao et al., 2018*). *Xie et al. (2011)* reported that H3K36me3 could recruit KDM5B to transcriptionally active intragenic regions to promote demethylation of H3K4me3. Few studies, however, have reported the regulatory role of *TFAP2C* in embryos on epitope-modifying enzymes. Our results showed that interference with *TFAP2C* affected gene expression of epigenetic modifying enzymes. H3K4me3 modification levels significantly decreased after *TFAP2C* interference. We inferred that it may be partly due to the demethylation activity of abnormally expressed KDM5B, and partly due to the recruitment of KDM5B by the overexpressed H3K36me3.

DNA methylation during the fertilization phase and post-fertilization period are of major importance for embryo development (*Anifandis et al., 2015*). It has

been shown that DNA methylation and histone modification interact with each other, and that the methylation of CpG islands related to the methylation status of H3K4 (*Zardo, 2021*) and the levels of methylated H3K4 (H3K4me3) tend to be inversely correlated with DNA methylation (*Okitsu and Hsieh, 2007*). Studies on *TFAP2C*-mediated DNA methylation changes, however, have not been reported. The results of the present study showed increased levels of 5 mC modifications in the two-cell and four-cell stages of IVF embryos after interference with *TFAP2C*. The modification level of H3K4me3 was decreased. This inverse trend is consistent with one of our previous studies (*Zhang et al., 2022*). In addition, DNMT1 expression seemed to be mostly in the nucleus of blastocysts lacking *TFAP2C*. It indicated that TFAP2C could affect DNA methylation level, which in turn affects embryonic development.

TFAP2C has been shown to play a role in pluripotent stem cell induction (*Pastor et al., 2018a*; *Wang et al., 2020a*). It has also been shown that a ternary complex of TFAP2C, oncoprotein Myc, and histone H3 (H3K4me3) demethylase KDM5B exists at the proximal promoter, thereby regulating *CDKN1A* expression to control the cell cycle (*Wong et al., 2012*). In pig embryos, *Lee et al. (2015)* reported that *OCT4* transcript levels were elevated in pig *TFAP2C*-KD eight-cell embryos and that *TFAP2C* may be involved in regulating *OCT4*; however, the investigators did not conduct further experiments to verify this regulatory relationship. In the present study, it is reported for the first time that *TFAP2C* could bind to the promoter region of *SETD2* to regulate its expression, and the two showed an inverse relationship. A previous study showed that *SETD2*-mediated levels of H3K36me3 were negatively related with levels of *EZH2*-catalyzed H3K27me3, suggesting that SETD2 can methylate EZH2 and promote EZH2 degradation (*Yuan et al., 2020*). Meanwhile, *SETD2*-catalyzed H3K36me3 modification is involved in crosstalk with other chromatin markers, including antagonism of H3K4me3 and H3K27me3, leading to de-novo DNA methylation through recruitment of DNA methyltransferases 3A and 3B (*Dhayalan et al., 2010*; *Xu et al., 2019*). Therefore, we speculate that, based on the results of the present study, *TFAP2C* interference causes elevated *SETD2* expression, which mediates increased H3K36me3 modification. Simultaneously increased *SETD2* caused degradation of *EZH2* on the one hand and recruited KDM5B for H3K4me3 demethylation on the other. Although a previous study reported that the knockdown of *SETD2* inhibited porcine embryonic development (*Shao et al., 2022*), our result showed that the high expression of *SETD2* was also not conducive to embryonic development, suggesting that the abnormal expression of *SETD2* was detrimental to embryonic development, and only appropriate *SETD2* gene expression level was beneficial to normal embryonic development. *TFAP2C* is a known markers of human ground-state naive pluripotency, and regulates germline cell formation (*Chen et al., 2018*); therefore, we hypothesize that *TFAP2C* also plays an important role in human embryonic development.

In conclusion, our results suggest that *TFAP2C* is a key transcriptional factor that regulates early embryo development in pigs. It can affect embryonic development by regulating epigenetic modifying enzymes, such as KDM5B, SETD2 and epigenetic modifications, such as H3K4me3, H3K36me3 and DNA methylation modifications. In addition, to the best of our knowledge, we report for the first time that the classical binding motif of TFAP2C can bind to the *SETD2* promoter region and regulate its expression, thus affecting embryonic developmental processes. These findings provide a theoretical basis for improving developmental efficiency and animal production.

DATA AVAILABILITY

We've put a link to the data in the manuscript.

ACKNOWLEDGEMENTS

This work was supported by National Natural Science Foundation (number: 31972874), Jilin Province Health Science and Technology Capacity Improvement Project (number: 2021JC006), Jilin Natural Science Foundation (number: YDZJ202201ZYTS445), Jilin Medical and Health Talents Project (number: JLSWSRCZX2021-112) in China.

AUTHORS' ROLES

ZL, DZ and SZ conceived and designed the research; DZ, DW and YZ conducted the research and acquired the data; DZ, MZ and QL analysed and interpreted the data; ZL, DZ, DW and XA wrote the manuscript. All authors were involved in drafting and revising the manuscript, and approval of the version to be submitted.

SUPPLEMENTARY MATERIALS

Supplementary material associated with this article can be found in the online version at doi:10.1016/j.rbmo.2023.103772.

REFERENCES

Anifandis, G, Messini, CI, Dafopoulos, K, Messinis, IE, 2015. Genes and Conditions Controlling Mammalian Pre- and Post-implantation Embryo Development. Curr Genomics 16, 32–46.

Aston, KI, Li, G-P, Hicks, BA, Winger, QA, White, KL., 2009. Genetic Reprogramming of Transcription Factor Ap-2γ in Bovine Somatic Cell Nuclear Transfer Preimplantation Embryos and Placentomes. Cloning and Stem Cells 11, 177–186.

Auman, HJ, Nottoli, T, Lakiza, O, Winger, Q, Donaldson, S, Williams, T, 2002. Transcription factor AP-2gamma is essential in the extra-embryonic lineages for early postimplantation development. Development 129, 2733–2747.

Bai, D, Sun, J, Chen, C, Jia, Y, Li, Y, Liu, K, Zhang, Y, Yin, J, Liu, Y, Han, X, Ruan, J, Kou, X, Zhao, Y, Wang, H, Wang, Z, Chen, M, Teng, X, Jiang, C, Gao, S, Liu, W., 2022. Aberrant H3K4me3 modification of epiblast genes of extraembryonic tissue causes placental defects and implantation failure in mouse IVF embryos. Cell Rep 39, 110784.

Bai, Q, Assou, S, Haouzi, D, Ramirez, JM, Monzo, C, Becker, F, Gerbal-Chaloin, S, Hamamah, S, De Vos, J., 2012. Dissecting the first transcriptional divergence during human embryonic development. Stem Cell Rev Rep 8, 150–162.

Bannister, AJ, Kouzarides, T., 2011. Regulation of chromatin by histone modifications. Cell Res 21, 381–395.

Barski, A, Cuddapah, S, Cui, K, Roh, TY, Schones, DE, Wang, Z, Wei, G, Chepelev, I, Zhao, K., 2007. High-resolution profiling of histone methylations in the human genome. Cell 129, 823–837.

Benevolenskaya, EV., 2007. Histone H3K4 demethylases are essential in development and differentiation. Biochem Cell Biol 85, 435–443.

Bernstein, BE, Mikkelsen, TS, Xie, X, Kamal, M, Huebert, DJ, Cuff, J, Fry, B, Meissner, A, Wernig, M, Plath, K, Jaenisch, R, Wagschal, A, Feil, R, Schreiber, SL, Lander, ES., 2006. A bivalent chromatin structure marks key developmental genes in embryonic stem cells. Cell 125, 315–326.

Chen, D, Liu, W, Zimmerman, J, Pastor, WA, Kim, R, Hosohama, L, Ho, J, Aslanyan, M, Gell, JJ, Jacobsen, SE, Clark, AT, 2018. The TFAP2C-Regulated OCT4 Naive Enhancer Is Involved in Human Germline Formation. Cell Rep 25, 3591-3602.e3595.

Chen, Z, Zhang, Y., 2020. Role of Mammalian DNA Methyltransferases in Development. Annu Rev Biochem 89, 135–158.

Dhayalan, A, Rajavelu, A, Rathert, P, Tamas, R, Jurkowska, RZ, Ragozin, S, Jeltsch, A, 2010. The Dnmt3a PWWP domain reads histone 3 lysine 36 trimethylation and guides DNA methylation. J Biol Chem 285, 26114–26120.

Diao YF, Lin T, Li X, Oqani RK, Lee JE, Kim SY, and Jin DI. Dynamic changes of SETD2, a histone H3K36 methyltransferase, in porcine oocytes, IVF and SCNT embryos. 2018; 13:e0191816.

Emura, N, Takahashi, K, Saito, Y, Sawai, K., 2019. The necessity of TEAD4 for early development and gene expression involved in differentiation in porcine embryos. J Reprod Dev 65, 361–368.

Hall, VJ, Christensen, J, Gao, Y, Schmidt, MH, Hyttel, P., 2009. Porcine pluripotency cell signaling develops from the inner cell mass to the epiblast during early development. Developmental Dynamics 238, 2014–2024.

Hashimoto, H, Vertino, PM, Cheng, X., 2010. Molecular coupling of DNA methylation and histone methylation. Epigenomics 2, 657–669.

Koch, CM, Andrews, RM, Flicek, P, Dillon, SC, Karaöz, U, Clelland, GK, Wilcox, S, Beare, DM, Fowler, JC, Couttet, P, James, KD, Lefebvre, GC, Bruce, AW, Dovey, OM, Ellis, PD, Dhami, P, Langford, CF, Weng, Z, Birney, E, Carter, NP, Vetrie, D, Dunham, I., 2007. The landscape of histone modifications across 1% of the human genome in five human cell lines. Genome Res 17, 691–707.

Kuckenberg, P, Kubaczka, C, Schorle, H., 2012. The role of transcription factor Tcfap2c/TFAP2C in trophectoderm development. Reprod Biomed Online 25, 12–20.

Lee, S-H, Kwon, J-W, Choi, I, Kim, N-H, 2016. Expression and function of transcription factor AP-2γ in early embryonic development of porcine parthenotes. Reproduction, Fertility and Development 28, 1197–1205.

Lee, SH, Kwon, JW, Choi, I, Kim, NH, 2015. Expression and function of transcription factor AP-2? in early embryonic development of porcine parthenotes. Reprod Fertil Dev.

Moore, LD, Le, T, Fan, G, 2013. DNA methylation and its basic function. Neuropsychopharmacology 38, 23–38.

Okitsu, CY, Hsieh, CL., 2007. DNA methylation dictates histone H3K4 methylation. Mol Cell Biol 27, 2746–2757.

Pastor WA, Liu W, Chen D, Ho J, Kim R, Hunt TJ, Lukianchikov A, Liu X, and Polo JM. TFAP2C regulates transcription in human naive pluripotency by opening enhancers. 2018a; 20:553-564.

Pastor, WA, Liu, W, Chen, D, Ho, J, Kim, R, Hunt, TJ, Lukianchikov, A, Liu, X, Polo, JM, Jacobsen, SE, Clark, AT, 2018b. TFAP2C regulates transcription in human naive pluripotency by opening enhancers. Nature Cell Biology 20, 553–564.

Shao, GB, Ding, HM, Gong, AH., 2008. Role of histone methylation in zygotic genome activation in the preimplantation mouse embryo. In Vitro Cell Dev Biol Anim 44, 115–120.

Shao W, Ning W, Liu C, Zou Y, Yao Y, Kang J, and Cao Z. Histone Methyltransferase SETD2 Is Required for Porcine Early Embryonic Development. 2022; 12.

Sharma, N, Kubaczka, C, Kaiser, S, Nettersheim, D, Mughal, SS, Riesenberg, S, Hölzel, M, Winterhager, E, Schorle, H., 2016. Tpbpa-Cre-mediated deletion of TFAP2C leads to deregulation of Cdkn1a, Akt1 and the ERK pathway, causing placental growth arrest. Development 143, 787–798.

Spitz, F, Furlong, EEM., 2012. Transcription factors: from enhancer binding to developmental control. Nature Reviews Genetics 13, 613–626.

Wang Y, Chen S, Jiang Q, Deng J, Cheng F, Lin Y, Cheng L, Ye Y, Chen X, Yao Y, Zhang X, Shi G, Dai L, Su X, and Peng Y. TFAP2C facilitates somatic cell reprogramming by inhibiting c-Myc-dependent apoptosis and promoting mesenchymal-to-epithelial transition. 2020a; 11:482.

Wang, Y, Chen, S, Jiang, Q, Deng, J, Cheng, F, Lin, Y, Cheng, L, Ye, Y, Chen, X, Yao, Y, Zhang, X, Shi, G, Dai, L, Su, X, Peng, Y, Deng, H., 2020b. TFAP2C facilitates somatic cell reprogramming by inhibiting c-Myc-dependent apoptosis and promoting mesenchymal-to-epithelial transition. Cell Death & Disease 11, 482.

Winger, Q, Huang, J, Auman, HJ, Lewandoski, M, Williams, T, 2006. Analysis of Transcription Factor AP-2 Expression and Function During Mouse Preimplantation Development1. Biol Reprod 75, 324–333.

Wong, P-P, Miranda, F, Chan KaYi, V, Berlato, C, Hurst Helen, C, Scibetta Angelo, G, 2012. Histone Demethylase KDM5B Collaborates with TFAP2C and Myc To Repress the Cell Cycle Inhibitor p21cip (CDKN1A). Molecular and cellular biology 32, 1633–1644.

Xie, L, Pelz, C, Wang, W, Bashar, A, Varlamova, O, Shadle, S, Impey, S., 2011. KDM5B regulates embryonic stem cell self-renewal and represses cryptic intragenic transcription. Embo j 30, 1473–1484.

Xu Q, Xiang Y, Wang Q, Wang L, Brind'Amour J, Bogutz AB, Zhang Y, Zhang B, Yu G, Xia W, Du Z, Huang C, Ma J, Zheng H, Li Y, Liu C, Walker CL, Jonasch E, and Lefebvre L. SETD2 regulates the maternal epigenome, genomic imprinting and embryonic development. 2019; 51:844-856.

Yuan, H, Han, Y, Wang, X, Li, N, Liu, Q, Yin, Y, Wang, H, Pan, L, Li, L, Song, K, Qiu, T, Pan, Q, Chen, Q, Zhang, G, Zang, Y, Tan, M, Zhang, J, Li, Q, Wang, X, Jiang, J, Qin, J., 2020. SETD2 Restricts Prostate Cancer Metastasis by Integrating EZH2 and AMPK Signaling Pathways. Cancer Cell 38, 350-365.e357.

Zaitseva, I, Zaitsev, S, Alenina, N, Bader, M, Krivokharchenko, A, 2007. Dynamics of DNA-demethylation in early mouse and rat embryos developed in vivo and in vitro. Mol Reprod Dev 74, 1255–1261.

Zardo, G., 2021. The Role of H3K4 Trimethylation in CpG Islands Hypermethylation in Cancer. Biomolecules 11.

Zhai, Y, Yu, H, An, X, Zhang, Z, Zhang, M, Zhang, S, Li, Q, Li, Z, 2022. Profiling the transcriptomic signatures and identifying the patterns of zygotic genome activation - a comparative analysis between early porcine embryos and their counterparts in other three mammalian species. BMC Genomics 23, 772.

Zhang, B, Zheng, H, Huang, B, Li, W, Xiang, Y, Peng, X, Ming, J, Wu, X, Zhang, Y, Xu, Q, Liu, W, Kou, X, Zhao, Y, He, W, Li, C, Chen, B, Li, Y, Wang, Q, Ma, J, Yin, Q, Kee, K, Meng, A, Gao, S, Xu, F, Na, J, Xie, W., 2016. Allelic reprogramming of the histone modification H3K4me3 in early mammalian development. Nature 537, 553–557.

Zhang, D, Zhou, Y, Huang, R, Zhai, Y, Wu, D, An, X, Zhang, S, Shi, L, Li, Q, Kong, X, Yu, H, Li, Z, 2022. LncRNA affects epigenetic reprogramming of porcine embryo development by regulating global epigenetic modification and the downstream gene SIN3A. Front Physiol 13, 971965.

Zhou, Q, Xiong, Y, Qu, B, Bao, A, Zhang, Y., 2021. DNA Methylation and Recurrent Pregnancy Loss: A Mysterious Compass? Front Immunol 12, 738962.

Received 8 September 2023; received in revised form 9 November 2023; accepted 12 December 2023.